Novel green activation processes and mechanism of peroxymonosulfate based on supported cobalt phthalocyanine catalyst

Zhenfu Huang, Haiwei Bao, Yuyuan Yao*, Wangyang Lu, Wenxing Chen**

National Engineering Lab of Textile Fiber Materials & Processing Technology (Zhejiang), Zhejiang Sci-Tech University, Hangzhou 310018, PR China

ABSTRACT

Catalytic activation of peroxymonosulfate (PMS) to generate radicals has received considerable and increasing attention in environmental catalysis field. The development of highly efficient and environmentally friendly oxidation processes has been one of the most important and greatly challenging goals in PMS activation field. Herein, an effective and stable catalyst (ACFs-CoPc) was proposed for PMS activation by supporting cobalt phthalocyanine (CoPc) onto activated carbon fibers (ACFs) covalently. With the dye of Acid Red 1 (AR1) as probe compound, ACFs-CoPc could effectively activate PMS to eliminate AR1, and the catalytic activity of ACFs-CoPc was almost not impaired during ten successive runs without detectable cobalt leaching, indicating that ACFs-CoPc/PMS system was a pro-environmental and efficient oxidation system. A hybrid method that combines electron paramagnetic resonance (EPR) technology with different radical scavengers effect on PMS activation was employed for the investigation of active species during the catalytic reaction. It was found that both hydroxyl and sulfate radical ($\cdot OH$, $SO_4{}^{\bullet-}$) were generated; importantly, $SO_4{}^{\bullet-}$ was speculated to serve as the dominant active species in the catalytic oxidation of AR1. Based on these results, a possible mechanism was proposed.

© 2014 Elsevier B.V. All rights reserved.

1. Introduction

The generation of active species, such as reactive oxygen species (ROS), is an important process in nature, occurring from human body to natural world [1]. Such active species have been widely investigated in various chemical areas, especially in catalysis field due to their high oxidative activity [2–4]. Sulfate radical ($SO_4{}^{\bullet-}$) has been known as one of the most powerful reactive oxygen species for its high standard redox potential (2.5–3.1 V) [5], which is comparable to that of hydroxyl radical ($\cdot OH$, 1.8–2.7 V) [6], and has attracted increasing attention for their high efficiency of oxidation of organic pollutants [7–9]. As one of the most efficient sources of $SO_4{}^{\bullet-}$, the activation of peroxymonosulfate (PMS) has been widely studied [10–12]. Recently, the most common catalysts for PMS activation are transition metals, with Co^{2+}/PMS system gives the best results of $SO_4{}^{\bullet-}$ generation [13,14]. However, employing Co^{2+} to active PMS under a homogeneous system will result in loss of Co, and since Co is recognized as a prior aqueous pollutant which can cause

several health problems such as asthma, pneumonia and other lung problems [15,16], the development of Co^{2+}/PMS homogeneous system has been restricted.

Therefore, the development of green possesses to generate $SO_4{}^{\bullet-}$ is highly desired on the basis of environmental consideration. On the one hand, developing heterogeneous Co catalysts for PMS activation is an efficient strategy to restrict the discharge of Co ion. Many efforts have been made on studies of heterogeneous Co catalysts, such as Co oxides [17,18], Co exchanged zeolites [19], Co-SBA-15 [20], or other supported Co catalysts [21,22]. However, Co ion leaching is still observed in different scales for many of them, which is regarded as a secondary pollution and loss of the catalyst. On the other hand, PMS activation by other transition metals with less environmental hazards, such as Fe catalysts, is considered as a relatively environmentally friendly technology [23,24]. However, most of these catalysts are generally not as efficient as Co catalysts in PMS activation. Thus, it is still a great challenge to balance the requirements of environmental friendliness and efficiency for PMS activation process.

Cobalt phthalocyanine (CoPc), which has a tetra N-donor macrocyclic structural similarity to the naturally occurring metalloporphyrin, has attracted a considerable interest as an oxidation catalyst because of its remarkable chemical and thermal stability

[25]. Compared with Co ion alone, the coordination of CoPc possesses attractive characteristics: (i) as CoPc has functional groups, such as amino, sulfo, and carboxyl in the peripheral benzene rings of the phthalocyanine structure, stable chemical bonds such as covalent bonds can be formed between CoPc and support to effectively restrict the loss of catalyst [26]; (ii) the catalytic properties of CoPc are facile to be tuned by the change of the substituent groups on the phthalocyanine ring [27]. However, CoPc as a homogeneous catalyst in aqueous solution is usually prone to aggregate at a relatively low concentration, negatively resulting in catalytically inactive dimers [28]. Moreover, the oxidative self-destruction of CoPc may occur in the catalytic oxidation, causing the loss of the catalyst. An efficient way to solve these problems is to immobilize it onto various supports, such as graphene [29], carbon nanotube [30], MCM-41 [31], chitosan [32] for improved catalytic ability and stability. Unfortunately, some of these catalysts such as CoPc-graphene, CoPc-carbon nanotube are inconvenient to separate from the reaction solution, which is likely to produce secondary pollution. Moreover, CoPc-MCM-41 exhibits unsatisfactory stability in recycling experiments, while CoPc-chitosan shows low effective catalytic activity. It is well known that excellent supports will bring excellent catalytic activity. Therefore, the selection of supports for CoPc is very significant to construct remarkable heterogeneous catalyst.

Compared with the above mentioned supports, activated carbon fibers (ACFs) have the potential of being an excellent support for the construction of heterogeneous CoPc catalysts because of its attractive features: (i) with a high surface area and microporous structure, ACFs have an extremely high adsorption capacity; (ii) as ACFs have plenty of active groups on the surface, they can provide a frame to anchor active sites for their stable immobilization and excellent dispersion on the support; (iii) the unusual chemical stability and inert structure can protect ACFs from the damage and improve the stability of the active sites under the attack of radicals in the oxidation reactions; (iv) ACFs can be confined in different textile structure, such as fiber tows, fabric and felts, aiding their handling. Based on afore considerations, we reported an efficient and stable heterogeneous catalyst, ACFs-CoPc, which was constructed by supporting CoPc onto ACFs via a covalent bond. This catalyst exhibited excellent catalytic activity for H_2O_2 activation for elimination of phenols, such as 4-nitrophenol [33]. However, the ACFs-CoPc/H_2O_2 system was almost ineffective for the degradation of dyes. In this work, we innovatively introduced PMS as the oxidant and used ACFs-CoPc as the activator of PMS to generate active species for the dyes elimination. To our best knowledge, it is the first report that supported CoPc catalyst is applied in PMS activation so far.

The primary concerns of this study were to verify the following questions: (i) can ACFs-CoPc effectively activate PMS to generate active species to catalytically oxidate dyes; (ii) can ACFs-CoPc be stable and reach the environmental friendly requirement during the activation process; (iii) what is the mechanism of PMS activation by ACFs-CoPc. Herein, Acid Red 1 (AR1) was selected as a probe compound to evaluate the catalytic activity of ACFs-CoPc for PMS activation. Electron paramagnetic resonance (EPR) technology combined with various radical scavengers has been employed to investigate the mechanism of PMS activation by ACFs-CoPc. It is expected that ACFs-CoPc/PMS system will open up a new area of potential research in the development of green oxidation processes.

2. Experimental

2.1. Materials and reagents

ACFs were purchased from Jiangsu Sutong Carbon Fiber Co., Ltd. (Jiangsu, China). Cobalt chloride hexahydrate, urea, ammonium molybdate, cyanuric chloride, and potassium peroxymonosulfate

(PMS: oxone, Aladdin Industrial Corporation) were used as analytical reagents. The spin trapping reagent 5,5-dimethyl-pyrroline-oxide (DMPO) was supplied from Tokyo Chemical Industry Co., Ltd. All dyes, including Acid Red 1 (AR1) and Reactive Brilliant Red M-3BE (RR M-3BE) are commercial compounds without further purification. Doubly distilled water was used throughout the dyes degradation process.

2.2. Preparation of ACFs-CoPc

CoPc with active groups was synthesized from cobalt teraaminophthalocyanine and cyanuric chloride according to the method described by Chen et al. [34]. ACFs were treated with acid for 12 h, washed with water to neutrality, and dried to obtain oxidated ACFs (o-ACFs). ACFs-CoPc was prepared by supporting CoPc to o-ACFs by covalent bond (see Supplementary Information for details of the process). The bonding site between CoPc and o-ACFs was investigated using X-ray photoelectron spectroscopy (Kratos Axis Ultra DLD, UK) and the results were shown in Fig. S1 (see Supplementary Information for details of the process).

2.3. Experimental procedures and analysis

The removal of dyes was carried out in a 40 mL glass beaker, with the temperature set at 50 °C using a constant temperature shaker water bath (DSHZ-300A, Taicang, Jiangsu). In all reactions, a reaction volume of 30 mL was used. A typical reaction mixture contained the following initial concentrations and amounts: the dyes (50 μM, except for MB (25 μM)), ACFs-CoPc (1 g/L), o-ACFs (1 g/L), PMS (0.6 mM). At given time intervals, the degradation efficiency of the dyes was determined by a UV-vis spectrometer (Hitachi U-3010) (see Supplementary Information for details of the process).

The cobalt ion content in the solution after the reaction was detected by an atomic adsorption spectrometer (Hitachi 170-70 atomic absorption spectrometer). EPR signals of radicals trapped by DMPO were recorded at ambient temperature on a Bruker A300 spectrometer. The settings for the EPR spectrometer were the following: center field, 3480 G; sweep width, 100 G; microwave frequency, 9.77 GHz; modulation frequency, 100 kHz; power, 12.72 mW.

3. Results and discussion

3.1. The catalytic activity of ACFs-CoPc

3.1.1. Oxidation removal of AR1

Control experiments were conducted to compare the eliminated efficiencies of AR1 by various processes with reaction temperature 50 °C, as presented in Fig. 1. With ACFs-CoPc only, a slight removal of AR1 was observed, and about 3% of AR1 was removed in 50 min (curve a), due to the adsorption of ACFs-CoPc. In the presence of PMS alone, about 14% of AR1 was degraded in 50 min (curve b). With addition of o-ACFs and PMS, AR1 elimination rate increased to 35%, while in the presence of ACFs-CoPc and PMS, fast and efficient degradation of AR1 was achieved, and nearly 100% of AR1 was degraded in 50 min, indicating that the introduction of CoPc to ACFs greatly enhanced the PMS activation and catalytic degradation of AR1. Besides, GC–MS analysis was performed to investigate the catalytic oxidation products of AR1. The possible structure of the intermediates and the methyl ester derivatives of the intermediates were given in Table S1. The residual products were identified including some small molecular biodegradable aliphatic carboxylic compounds such as oxalic acid, fumaric acid, adipic acid. The results show that ACFs-CoPc is an efficient catalyst for oxidation elimination of AR1 in the presence of PMS. Furthermore, compared with the efficiency of AR1 degradation by ACFs-CoPc/H_2O_2 system
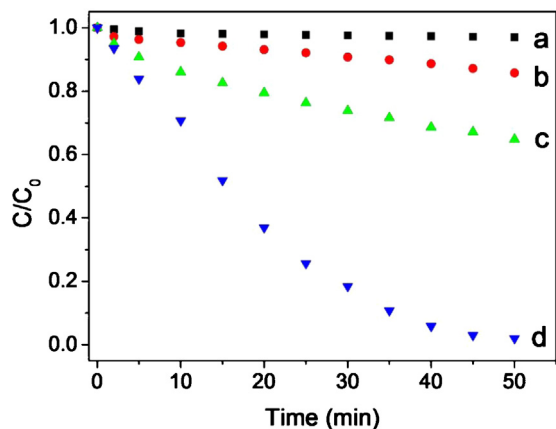
Fig. 1. Concentration changes of AR 1 under different conditions: (a) ACFs-CoPc; (b) PMS; (c) o-ACFs, PMS; (d) ACFs-CoPc, PMS (the dosage of ACFs-CoPc or o-ACFs: 1 g/L; [AR 1]$_0$: 50 μM; [PMS]$_0$: 0.6 mM; T = 50 °C; pH 6.66).

(Fig. S2), ACFs-CoPc/PMS system provided a much higher efficiency and showed a great potential value in the dyes effluent treatment.

3.1.2. Reuse of ACFs-CoPc

In addition, successive batches of AR1 degradation under standard reaction conditions were conducted to investigate the reusability of ACFs-CoPc, which was a significant concern for a heterogeneous catalyst for its application. The catalyst was taken out after each cycle experiment and rinsed with deionized water to remove the residual PMS, and dried at 60 °C. This above process was repeated ten times. The results in Fig. 2 show that the degradation rate of AR1 remained similar in ten successive runs, implying that the activity of ACFs-CoPc was almost not impaired in repetitive experiments. Moreover, atomic absorption spectroscopy was used to detect whether there was any free cobalt ion in the aqueous solution after the reaction. As expected, no detectable amount of dissolved Co could be measured during the ten successive oxidation processes, indicating that ACFs-CoPc was relatively stable in the catalytic reaction. To further confirm the stability of ACFs-CoPc, FT-IR spectra were employed to investigate the structural change of ACFs-CoPc before and after catalytic reaction, as shown in Fig. S3. As expected, after ten runs, the IR spectra of ACFs-CoPc almost remained the same as that before the reaction, suggesting that the CoPc on ACFs were almost not impaired during the reaction. However, CoPc alone was not stable enough and was facile to be self-destructed by PMS (Fig. S4). These afore results indicate that the introduction of ACFs could efficiently improve the stability
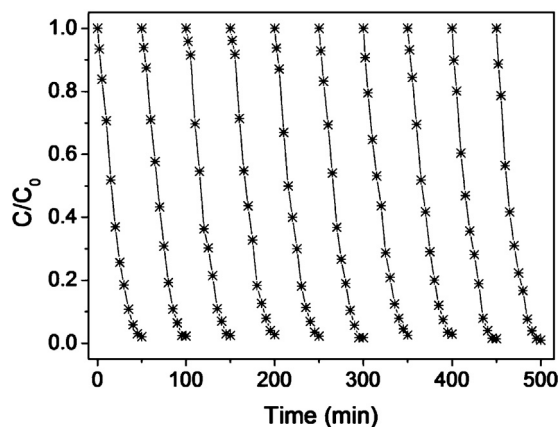

Fig. 2. Repeated recycling of ACFs-CoPc with PMS for the degradation of AR 1 (the dosage of ACFs-CoPc: 1 g/L; [AR 1]$_0$: 50 μM; [PMS]$_0$: 0.6 mM; T = 50 °C; pH 6.66).
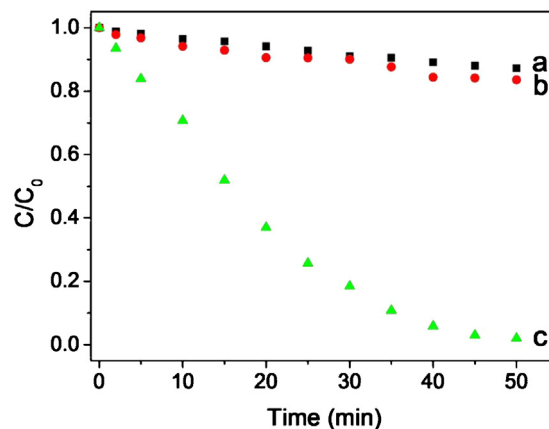

Fig. 3. Influence of ascorbic acid to the AR 1 degradation by the PMS activation with ACFs-CoPc: (a) ACFs-CoPc, ascorbic acid; (b) ACFs-CoPc, PMS, ascorbic acid; (c) ACFs-CoPc, PMS (the dosage of ACFs-CoPc: 1 g/L; [AR 1]$_0$: 50 μM; [PMS]$_0$: 0.6 mM; T = 50 °C; pH 6.66).

of CoPc, and the supported catalyst of ACFs-CoPc remained almost intact in repetitive utilization, consistent with the results in Fig. 2. Therefore, ACFs-CoPc is more environmentally friendly than most supported cobalt catalysts for PMS activation.

3.2. Catalytic oxidation mechanism

3.2.1. Identification of active species

To test whether radical species were generated in the ACFs-CoPc/PMS system, first of all, ascorbic acid, a popular radical scavenger [35,36], was added to the reaction solution to investigate whether the AR1 degradation could be inhibited. As shown in Fig. 3, rapid removal of AR1 was achieved by ACFs-CoPc/PMS system, and nearly 100% of AR1 was removed in 50 min. Significantly, in the control experiment with the addition of 0.02 M ascorbic acid, the removal rate of AR1 sharply decreased to 16%, which was almost the same compared to the elimination of AR1 without PMS, implying that the addition of ascorbic acid almost completely inhibited the degradation of AR1. It can be preliminarily concluded that radical species played a major role in the ACFs-CoPc mediated degradation, which is different from the reported non-radical mechanism of ACFs-CoPc/H$_2$O$_2$ in our previous work [33]. In the activation of PMS, the sulfate radical (SO$_4^{•-}$) is the well-accepted key active species for pollutant degradation [10,37,38]. Therefore, electron paramagnetic resonance (EPR) was utilized to investigate whether SO$_4^{•-}$ was generated in the catalytic reaction and 5,5-dimethyl-pyrroline-oxide (DMPO) was used as the spin trapping reagent. From EPR spectra (Fig. 4), ACFs-CoPc/PMS system could form typical DMPO-SO$_4$ and DMPO-OH signals based on their hyperfine splitting constants (DMPO-SO$_4$: α_N = 13.2 G, α_H = 9.6 G, α_H = 1.48 G, and α_H = 0.78 G; DMPO-OH: α_H = α_N = 14.9 G), while no detectable signals could be measured in the mixing of ascorbic acid and ACFs-CoPc/PMS system, which was in agreement with the removal result in Fig. 3, indicating that both SO$_4^{•-}$ and $^{•}$OH were generated.

To evaluate the contribution of two radical species to AR1 degradation, two radical scavengers, methanol (MA) and tert-butyl alcohol (TBA), were employed. Containing α-hydrogen, MA was used as a probe compound for the total flux of hydroxyl and sulfate radical because of its high reactivity with both hydroxyl and sulfate radical ($k_{•OH}$: 9.7 × 10^8 M^{-1} s^{-1}; $k_{SO_4^{•-}}$: 3.2 × 10^6 M^{-1} s^{-1}) [6,39]. Without α-hydrogen, TBA has much different reaction rate constants, and it was preferably used as a hydroxyl radical-specific probe because of its high reactivity with hydroxyl radicals ($k_{•OH}$: (3.8–7.6) × 10^8 M^{-1} s^{-1}) but relatively lower reactivity with sulfate radical than that with MA ($k_{SO_4^{•-}}$: (4–9.1) × 10^5 M^{-1} s^{-1}) [13].
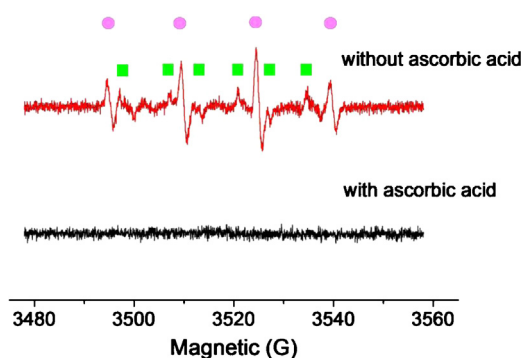
Fig. 4. EPR spectra of PMS with or without ascorbic acid at 5 min ([ascorbic acid]$_0$: 0.02 M; the dosage of ACFs-CoPc: 1 g/L; [AR 1]$_0$: 50 μM; [PMS]$_0$: 0.6 mM; T = 50 °C; pH 6.66). ■ (green): DMPO-SO$_4$; ● (pink): DMPO-OH. (For interpretation of the references to color in this figure legend, the reader is referred to the web version of the article.)

Therefore, the scavengers, TBA and MA, were used to identify which was the dominant radical special responsible for AR1 degradation. In Fig. 5, with addition of 0.22 M TBA, a significant decrease in degradation rate of AR1 was observed, and the removal rate decreased from 16%, 30%, and 82% to 7%, 15%, and 52% at 5, 10, and 30 min, respectively. In the case of MA (0.22 M) addition, a relatively greater drop was observed during the degradation process compared to that of TBA addition, and the degradation rate was 6%, 15%, and 27% at 5, 10, and 30 min, preliminary speculating that SO$_4^{\bullet-}$ predominately decomposed AR1 over $^\bullet$OH during the catalytic oxidation.

Furthermore, to investigate the $^\bullet$OH and SO$_4^{\bullet-}$ mediated in the PMS activation process, the influence of different scavengers, MA and potassium iodide (KI), on the degradation of AR1 was determined. Excess MA (2.2 M) was added to the solution to scavenger all $^\bullet$OH and SO$_4^{\bullet-}$ (including surface-bound radicals and free radicals) generated in the system, while excess KI (10 mM) was used to scavenger all the surface-bound $^\bullet$OH and SO$_4^{\bullet-}$ ($^\bullet$OH$_{ads}$ and SO$_4^{\bullet-}$$_{ads}$) produced at the surface of ACFs-CoPc [40–42]. As it can be seen in Fig. 6, in the presence of MA, only about 14% of AR1 was removed in 50 min by ACFs-CoPc/PMS system, implying that the removal of AR1 was almost completely inhibited by MA. With the addition of KI, the degradation of AR1 decreased from 16%, 30%, and 82% to 8%, 13%, and 23% at 5, 10 and 30 min, respectively, indicating that $^\bullet$OH$_{ads}$ and SO$_4^{\bullet-}$$_{ads}$ played a dominant role and only a minimal amount of free $^\bullet$OH and SO$_4^{\bullet-}$ ($^\bullet$OH$_{free}$ and SO$_4^{\bullet-}$$_{free}$) existed in the catalytic oxidation reaction.
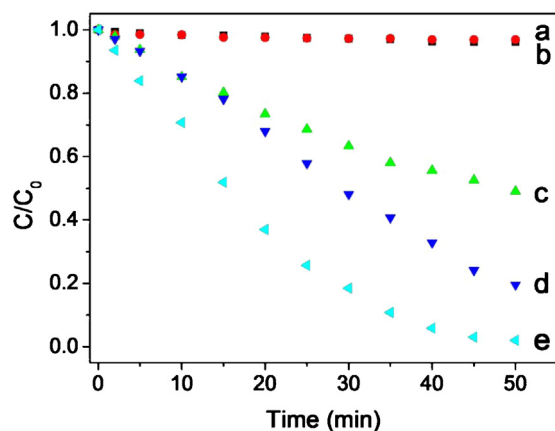

Fig. 5. Effect of methanol (MA) and tert-butyl alcohol (TBA) to the AR 1 degradation by the PMS activation with ACFs-CoPc: (a) ACFs-CoPc, MA; (b) ACFs-CoPc, TBA; (c) ACFs-CoPc, MA, PMS; (d) ACFs-CoPc, TBA, PMS; (e) ACFs-CoPc, PMS ([MA]$_0$ and [TBA]$_0$: 0.22 M; the dosage of ACFs-CoPc: 1 g/L; [AR 1]$_0$: 50 μM; [PMS]$_0$: 0.6 mM; T = 50 °C; pH 6.66).
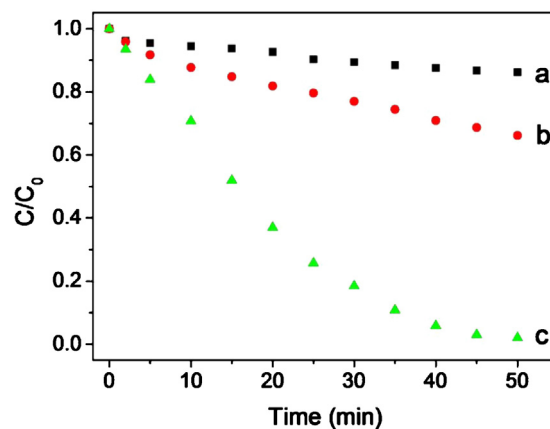

Fig. 6. Influence of methanol (MA) and potassium iodide (KI) on the AR 1 degradation: (a) ACFs-CoPc, MA, PMS; (b) ACFs-CoPc, KI, PMS; (c) ACFs-CoPc, PMS ([MA]$_0$: 2.2 M; [KI]$_0$: 10 mM; the dosage of ACFs-CoPc: 1 g/L; [AR 1]$_0$: 50 μM; [PMS]$_0$: 0.6 mM; T = 50 °C; pH 6.66).

3.2.2. Effects of PMS concentration and catalyst dosage on radicals

Afore experimental results show both SO$_4^{\bullet-}$ and $^\bullet$OH existed in the ACFs-CoPc/PMS system. It is absolutely indispensable to further investigate the effects of PMS concentration and catalyst dosage on the variation of SO$_4^{\bullet-}$ and $^\bullet$OH, which are favorable to analyze the catalytic oxidation process and mechanism. The effect of PMS concentration on the degradation of AR1 and the variation of SO$_4^{\bullet-}$ and $^\bullet$OH were shown in Fig. 7. From Fig. 7A, with the increase of PMS concentration from 0.15 mM to 2.4 mM, the degradation rate raised rapidly from 10%, 37% to 79%, 98% at 10, 30 min, respectively, indicating that PMS with higher concentration provides relatively better degradation efficiency. Moreover, EPR was used to investigate the radicals variation at different reaction time with various PMS concentrations (detailed EPR spectra are shown in Fig. S5), and the peak intensity of DMPO-radical adducts is utilized to represent the concentration of radical species. Fig. 7B shows the plots of peak intensity of DMPO-OH versus reaction time. When the PMS concentration was between 0.15 and 0.6 mM, the peak intensity of DMPO-OH increased with the increase of PMS concentration. However, to our surprise, when the PMS concentration went up to 1.2 and 2.4 mM, the peak intensity of DMPO-OH decreased with the increase of PMS concentration, which might be ascribed to the reaction between $^\bullet$OH and PMS to generate SO$_4^{\bullet-}$ [43]. Meanwhile, the peak intensity of DMPO-SO$_4$ increased with the increase of PMS concentration from 0.15 to 0.6 mM (Fig. 7C). When the PMS concentration was 1.2 and 2.4 mM, the peak intensity of DMPO-SO$_4$ first increased and then decreased with the reaction time prolonged. Based on the afore phenomena, we speculated that the sharp decrease of the peak intensity of DMPO-SO$_4$ was ascribed to the formation of nitroxide radical (5,5-dimethylpyrrolidone-(2)-oxyl-(1), DMPOX). Therefore, EPR was used to detect the existence of DMPOX, as shown in Fig. S5 (d and e). It was obviously seen that a set of characteristic signals appeared in EPR spectra, which was assigned to the peak of DMPOX [44], and even the peak intensity of DMPOX almost increased with increasing reaction time (Fig. 7D), suggesting that it was quite in accordance with our speculation. Importantly, it was observed with 0.15 mM PMS and ACFs-CoPc in the solution, only DMPO-OH was detected while no characteristic peak of DMPO-SO$_4$ was observed (Fig. S5(a)), indicating that $^\bullet$OH was initially generated in the activation of PMS by ACFs-CoPc.

The effect of ACFs-CoPc dosage on the degradation of AR1 and the variation of SO$_4^{\bullet-}$ and $^\bullet$OH was further investigated, as shown in Fig. 8. As observed in Fig. 8A, with the dosage of ACFs-CoPc increased from 0.1 g/L to 5 g/L, the removal rate of AR1 at 5, 10,
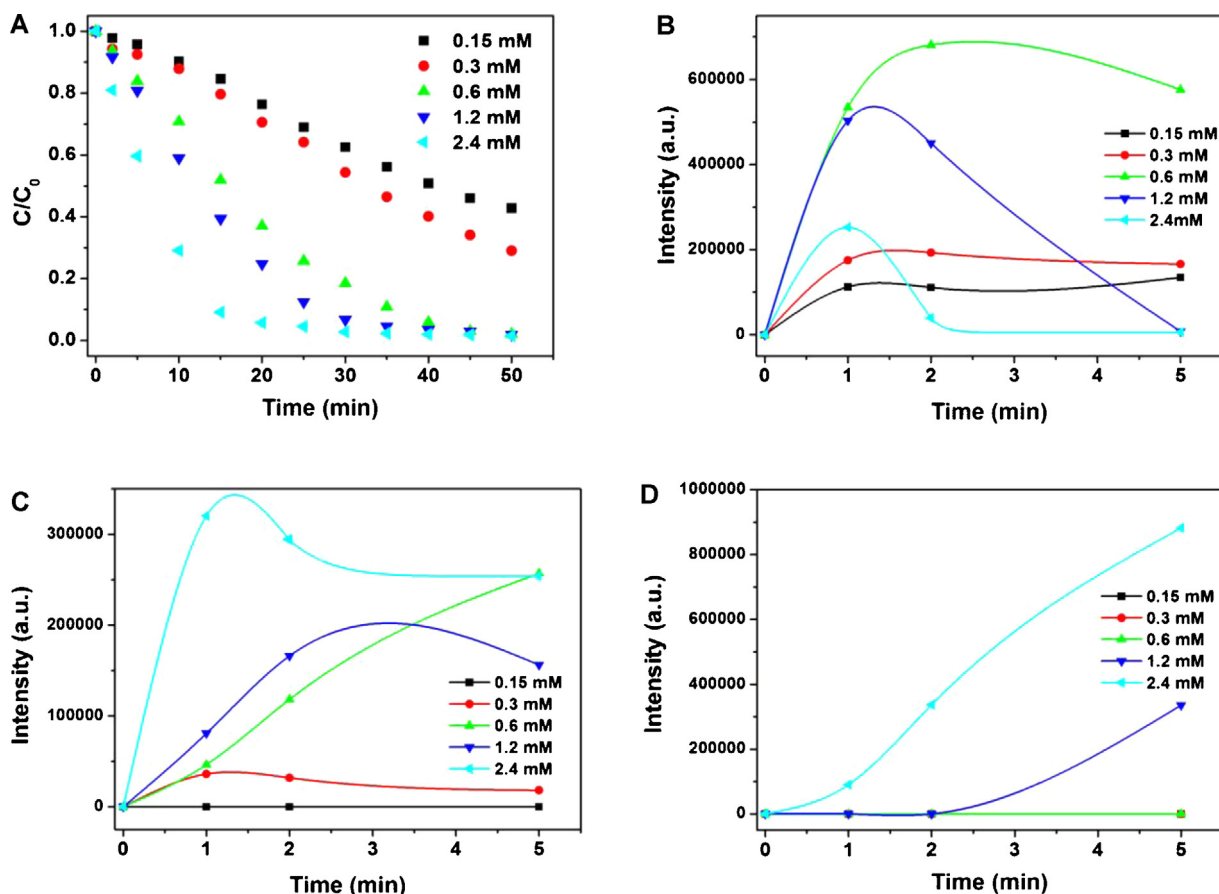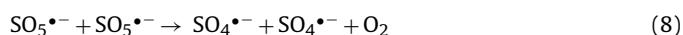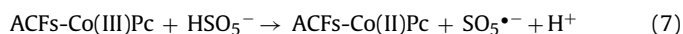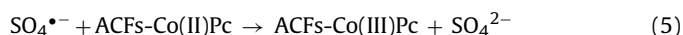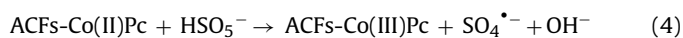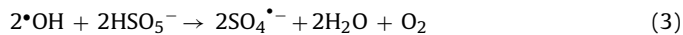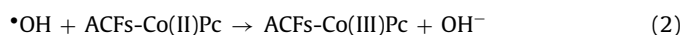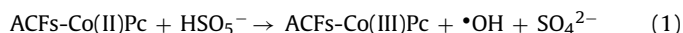
Fig. 7. Effects of PMS concentration on the AR 1 degradation: (A) concentration changes of AR 1; (B) changes in intensity of DMPO-OH; (C) changes in intensity of DMPO-SO$_4$; (D) changes in intensity of DMPOX ([DMPO]$_0$: 10 mM; the dosage of ACFs-CoPc: 1 g/L; [AR 1]$_0$: 50 μM; [PMS]$_0$: 0.6 mM; T = 50 °C; pH 6.66).

and 30 min increased from and 3%, 5%, and 17% to 18%, 36%, and 86%, respectively, suggesting that the AR1 degradation could be accelerated by the increase of ACFs-CoPc dosage. Furthermore, the generation of •OH and SO$_4$•$^-$ during the catalytic oxidation process was investigated by EPR (detailed EPR spectra are shown in Fig. S6). From Fig. 8B, when the dosage of ACFs-CoPc was from 0.1 g/L to 0.5 g/L, the peak intensity of DMPO-OH increased with the increase of ACFs-CoPc dosage. However, with increase of ACFs-CoPc dosage up to 1 and 5 g/L, the peak intensity of DMPO-OH decreased with the increase of ACFs-CoPc dosage. Meanwhile, with the dosage of ACFs-CoPc increased from 0.1 to 1 g/L, the peak intensity of DMPO-SO$_4$ almost increased with the increase of ACFs-CoPc dosage and reaction time (Fig. 8C). However, when the ACFs-CoPc dosage was 5 g/L, the peak intensity of DMPO-SO$_4$ first increased and then decreased with increasing reaction time. The above results were nearly consistent with Fig. 7C, further confirmed by Fig. 8D, in which the peak intensity of DMPOX almost increased with increasing reaction time. Importantly, in the presence of 0.1 g/L ACFs-CoPc and PMS, similar to Fig. S5 (a), only DMPO-OH was detected while no characteristic peak of DMPO-SO$_4$ was observed within 2 min (Fig. S6 (a)), which further confirms that •OH was initially generated in the catalytic oxidation.

3.2.3. Analysis of catalytic oxidation process and mechanism

Based on these results mentioned above, main processes during the catalytic activation of PMS are proposed as follows. First, ACFs-Co(II)Pc activated PMS to generate •OH (Eq. (1)), but depleted •OH through Eq. (2). Some initially generated •OH species reacted with PMS to generate SO$_4$•$^-$ (Eq. (3)). Moreover, ACFs-Co(II)Pc could activate PMS to produce SO$_4$•$^-$ (Eq. (4)), while a part of

SO$_4$•$^-$ species were consumed (Eqs. (5) and (6)). Meanwhile, ACFs-Co(III)Pc reacted with PMS, which leaded to the recovery of the original ACFs-Co(II)Pc and the generation of SO$_4$•$^-$ and •OH (Eqs. (7)–(9)). Moreover, there were some competitive reactions that could negatively affect the generation of radicals, as seen in Eqs. (10)–(12). Furthermore, AR1 in aqueous solution was enriched continuously on the surface of ACFs-CoPc and broken down by SO$_4$•$^-$ and •OH. Herein, a possible mechanism of AR1 degradation by ACFs-CoPc/PMS system is proposed in Fig. 9.

$$\text{ACFs-Co(II)Pc} + \text{HSO}_5^- \rightarrow \text{ACFs-Co(III)Pc} + {}^{\bullet}\text{OH} + \text{SO}_4^{2-} \tag{1}$$

$${}^{\bullet}\text{OH} + \text{ACFs-Co(II)Pc} \rightarrow \text{ACFs-Co(III)Pc} + \text{OH}^- \tag{2}$$

$$2{}^{\bullet}\text{OH} + 2\text{HSO}_5^- \rightarrow 2\text{SO}_4^{\bullet-} + 2\text{H}_2\text{O} + \text{O}_2 \tag{3}$$

$$\text{ACFs-Co(II)Pc} + \text{HSO}_5^- \rightarrow \text{ACFs-Co(III)Pc} + \text{SO}_4^{\bullet-} + \text{OH}^- \tag{4}$$

$$\text{SO}_4^{\bullet-} + \text{ACFs-Co(II)Pc} \rightarrow \text{ACFs-Co(III)Pc} + \text{SO}_4^{2-} \tag{5}$$

$$\text{SO}_4^{\bullet-} + \text{OH}^- \rightarrow {}^{\bullet}\text{OH} + \text{SO}_4^{2-} \tag{6}$$

$$\text{ACFs-Co(III)Pc} + \text{HSO}_5^- \rightarrow \text{ACFs-Co(II)Pc} + \text{SO}_5^{\bullet-} + \text{H}^+ \tag{7}$$

$$\text{SO}_5^{\bullet-} + \text{SO}_5^{\bullet-} \rightarrow \text{SO}_4^{\bullet-} + \text{SO}_4^{\bullet-} + \text{O}_2 \tag{8}$$

$$2\text{SO}_5^{\bullet-} + 2\text{OH}^- \rightarrow 2\text{SO}_4^{2-} + 2{}^{\bullet}\text{OH} + \text{O}_2 \tag{9}$$

$${}^{\bullet}\text{OH} + {}^{\bullet}\text{OH} \rightarrow \text{H}_2\text{O}_2 \tag{10}$$

$$\text{SO}_4^{\bullet-} + \text{SO}_4^{\bullet-} \rightarrow \text{S}_2\text{O}_8^{2-} \tag{11}$$

$${}^{\bullet}\text{OH} + \text{SO}_4^{\bullet-} \rightarrow \text{HSO}_5^- \tag{12}$$
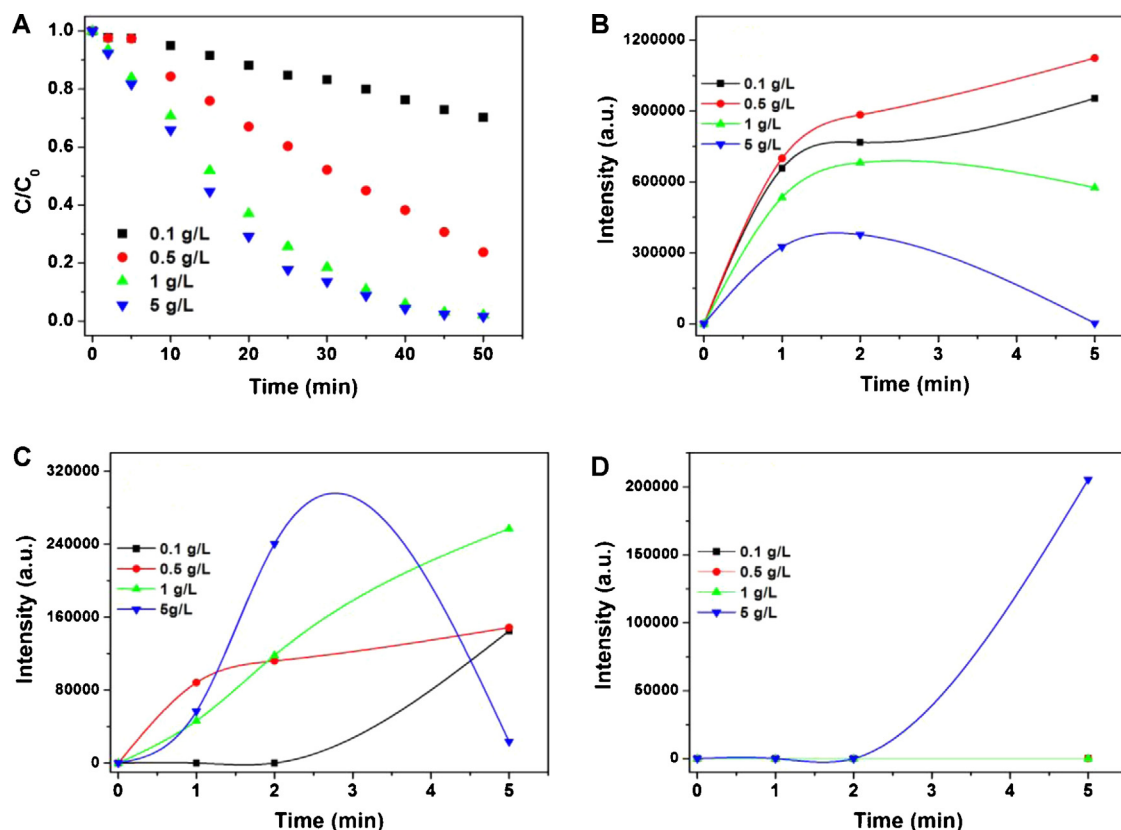
Fig. 8. Effects of ACFs-CoPc dosage on the AR 1 degradation: (A) concentration changes of AR 1; (B) changes in intensity of DMPO-OH; (C) changes in intensity of DMPO-SO$_4$; (D) changes in intensity of DMPOX ([DMPO]$_0$: 10 mM; the dosage of ACFs-CoPc: 1 g/L; [AR 1]$_0$: 50 μM; [PMS]$_0$: 0.6 mM; T = 50 °C; pH 6.66).

3.2.4. Effect of adsorption process on dyes degradation

The above findings hint that surface-bound radicals played the dominant role in the AR1 degradation, and dyes were firstly adsorbed to the surface of the supported catalyst and degraded in situ in the presence of PMS. During the whole catalytic oxidation process for eliminating dyes, the adsorption and catalytic oxidation facilitated one another, greatly promoting the catalytic degradation process, implying that the ACFs played an important
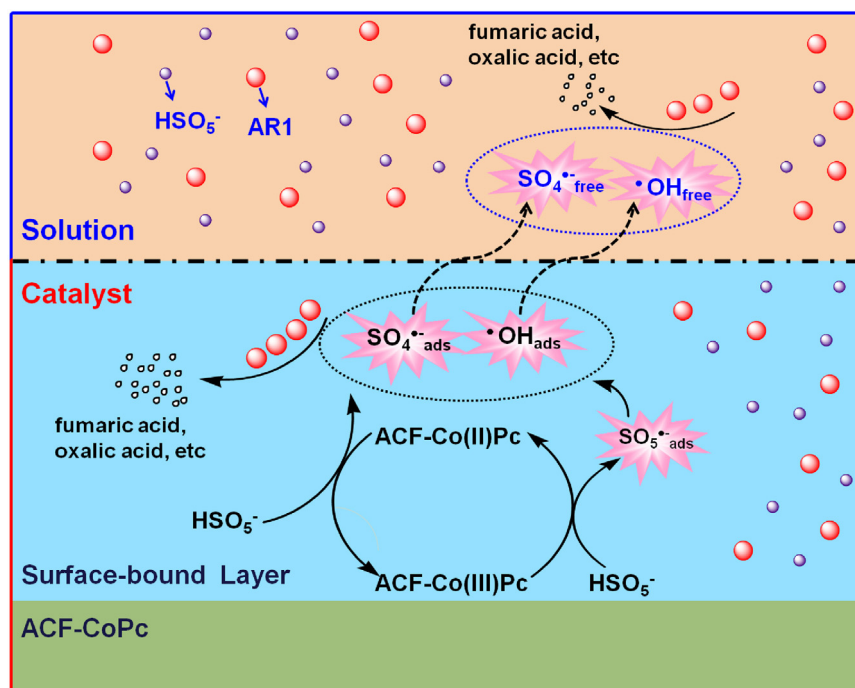

Fig. 9. The proposed mechanism of the PMS activation by ACFs–CoPc for AR 1 degradation.
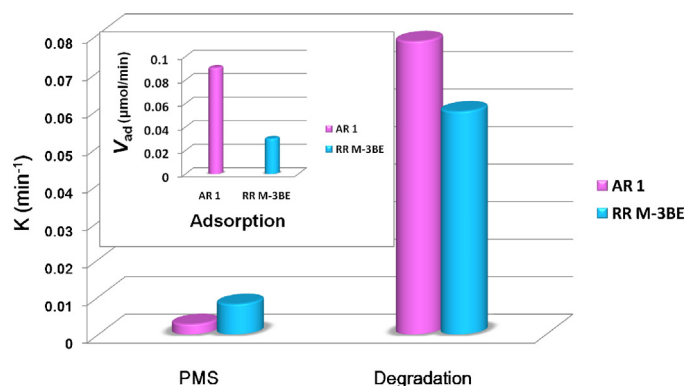
Fig. 10. The comparison of apparent pseudo-first-order kinetic constants between AR 1 and RR M-3BE degradation by ACFs-CoPc/PMS system. The inset: the adsorption rate of AR 1 and RR M-3BE by ACFs-CoPc/PMS system (the dosage of ACFs-CoPc: 1 g/L; $[AR 1]_0$: 50 μM; $[RR M-3BE]_0$: 50 μM; $[PMS]_0$: 0.6 mM; $T = 50 ℃$; pH 6.66).

role during the entire catalytic degradation process. Therefore, it is absolutely indispensable to further investigate the effects of the adsorption of ACFs on the catalytic oxidation performance. Herein, we designed two experiments to differentiate the adsorption and catalytic oxidation. Two dyes, AR1 and Reactive Brilliant Red M-3BE (RR M-3BE), having different adsorption rate on ACFs-CoPc, were used as the probe compounds. The adsorption rate (v_{ad}) is evaluated by plotting adsorbing quantity against time in 50 min, and the elimination rates of the reaction by only PMS (k_{PMS}) or ACFs-CoPc/PMS ($k_{ACFs-CoPc/PMS}$) are evaluated by apparent pseudo-first-order kinetic constants. As shown in Fig. 10, v_{ad} for AR1 is 0.00090 μmol/min, which is about three times as that for RR M-3BE (0.00030 μmol/min), suggesting that AR1 is more easily adsorbed by ACFs-CoPc than RR M-3BE. With PMS alone, the k_{PMS} of AR1 (0.00269 min^{-1}) is about one third as that of RR M-3BE (0.00804 min^{-1}), indicating that AR1 is relatively harder to be decomposed than RR M-3BE in a certain degree. Surprisingly, in ACFs-CoPc/PMS system, the $k_{ACFs-CoPc/PMS}$ of AR1 (0.07806 min^{-1}) is higher than that of RR M-3BE (0.05939 min^{-1}), indicating that the adsorption process plays an important role in the dyes degradation. The above experimental results indicated that a high adsorption rate was favorable to the improvement of dyes degradation efficiency. In this way, dyes could be enriched quickly onto ACFs-CoPc and in situ decomposed, which was consistent with the proposed mechanism.

From the afore analysis, it was obviously seen that a higher adsorption capacity of ACFs-CoPc to dyes brings a better catalytic degradation efficiency. In fact, the surface structure of ACFs-CoPc is the most important factor to affect the adsorption capacity, so we investigated how the surface structure of ACFs-CoPc affected the catalytic degradation performance. Before the catalytic elimination of dyes, ACFs-CoPc was immersed into the dyes solution to adsorb part of dyes to change the surface structure of ACFs-CoPc, and the process was denoted as the preadsorption. The ACFs-CoPc treated by the preadsorption was used to catalytically degrade the dyes in order to further investigate the effect of the adsorption capacity on the catalytic ability. Therefore, ACFs-CoPc was treated by immersing into the dyes solution for 10, 30, and 50 min, respectively, which would adsorb different contents of dyes (Table S2), and then pretreated ACFs-CoPc was taken out and immersed into the catalytic system. The influence of preadsorption on the dyes degradation is evaluated by plotting $k_{ACFs-CoPc/PMS}$ against preadsorbed content (adsorption dyes content onto ACFs-CoPc). In Fig. 11A, when the preadsorbed content increased from 0 to 1.506 μmol/g, the $k_{ACFs-CoPc/PMS}$ of AR1 by ACFs-CoPc/PMS system increased from 0.07806 to 0.16212 min^{-1}. To explain the phenomenon, pH at the point of zero charge (pH$_{pzc}$) of treated
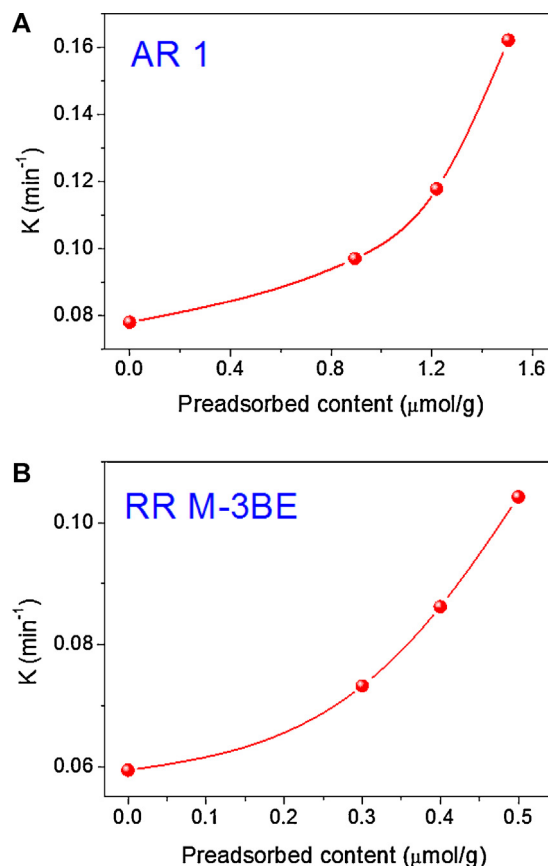

Fig. 11. Effect of preadsorbed content on apparent pseudo-first-order kinetic constants of different dyes degradation: (A) AR 1; (B) RR M-3BE (the dosage of ACFs-CoPc: 1 g/L; $[AR 1]_0$: 50 μM; $[RR M-3BE]_0$: 50 μM; $[PMS]_0$: 0.6 mM; $T = 50 ℃$; pH 6.66).

ACFs-CoPc was investigated, as show in Fig. S7. And the pH$_{pzc}$ of ACFs-CoPc increased after the preadsorption treatment in AR1 solution, meaning that the Zeta (ζ) electric potential increased in AR1 solution at the same pH, indicating that the transfer of these electronegative dyes from aqueous phase to fiber phase was more convenient and the adsorption process was accelerated [45], thus facilitating the catalytic oxidation. Moreover, the preadsorption treatment of ACFs-CoPc in RR M-3BE solution was investigated. Similar phenomenon was observed, with the preadsored content of RR M-3BE increased from 0 to 0.5 μmol/g, the $k_{ACFs-CoPc/PMS}$ increased nearly 1-fold to 0.10424 min^{-1} (Fig. 11B). These results indicated that the preadsorption process specially contribute to the acceleration of catalytically elimination of dyes. The finding might provide the potential for ACFs-CoPc/PMS system in the treatment of contaminants with low concentration, such as pharmaceuticals and personal care products.

4. Conclusion

In summary, this study demonstrates that the use of ACFs-CoPc as a heterogeneous catalyst for PMS activation is promising. Of particular interests for the work here are as follows: (i) PMS could be effectively activated by ACFs-CoPc to eliminate dyes; (ii) ACFs-CoPc exhibited excellent catalytic activity and remarkable reusability, more importantly, Co ion was almost not detected during catalytic reaction, indicating that ACFs-CoPc/PMS is a green and highly efficient catalytic technology; (iii) Both $^{\bullet}OH_{ads}$ and $SO_4^{\bullet-}{}_{ads}$ were generated in the catalytic reaction, importantly, $SO_4^{\bullet-}{}_{ads}$ was speculated to serve as the dominant active species. This work provides

a new approach to solve the contradiction between the efficiency and pro-environment in PMS activation. We hope that this paper may act as a catalyst in boosting the development of highly efficient and green oxidation technology based on PMS activation process and its application in environmental remediation.

Acknowledgments

Appendix A. Supplementary data

Supplementary data associated with this article can be found, in the online version, at http://dx.doi.org/10.1016/j.apcatb.2014.02.005.

References

[1] G. Herzberg, The Spectra and Structures of Simple Free Radicals: An Introduction to Molecular Spectroscopy, Dover Publications, Inc., Mineola, NY, 2003.
[2] J. Criquet, N.K.V. Leitner, Chemosphere 77 (2009) 194–200.
[3] B.C. Gau, H. Chen, Y. Zhang, M.L. Gross, Anal. Chem. 82 (2010) 7821–7827.
[4] X. Yang, X. Xu, J. Xu, Y. Han, J. Am. Chem. Soc. 135 (2013) 16058–16061.
[5] P. Neta, R.E. Huie, A.B. Ross, J. Phys. Chem. Ref. Data 17 (1988) 1027–1284.
[6] G.V. Buxton, C.L. Greenstock, W.P. Helman, A.B. Ross, J. Phys. Chem. Ref. Data 17 (1988) 513–531.
[7] H. Sun, S. Liu, G. Zhou, H.M. Ang, M.O. Tadé, S. Wang, ACS Appl. Mater. Interface 4 (2012) 5466–5471.
[8] Y. Ding, L. Zhu, N. Wang, H. Tang, Appl. Catal. B: Environ. 129 (2013) 153–162.
[9] G. Fang, J. Gao, D.D. Dionysiou, C. Liu, D. Zhou, Environ. Sci. Technol. 47 (2013) 4605–4611.
[10] E. Saputra, S. Muhammad, H. Sun, H.-M. Ang, M.O. Tadé, S. Wang, Appl. Catal. B: Environ. 142–143 (2013) 729–735.
[11] H. Sun, Y. Wang, S. Liu, L. Ge, L. Wang, Z. Zhu, S. Wang, Chem. Commun. 49 (2013) 9914–9916.
[12] E. Saputra, S. Muhammad, H. Sun, H.M. Ang, M.O. Tadé, S. Wang, Environ. Sci. Technol. 47 (2013) 5882–5887.
[13] G.P. Anipsitakis, D.D. Dionysiou, Environ. Sci. Technol. 38 (2004) 3705–3712.
[14] P.R. Shukla, S.B. Wang, H.M. Ang, M.O. Tadé, Sep. Purif. Technol. 70 (2010) 338–344.
[15] S.K. Ling, S.B. Wang, Y.L. Peng, J. Hazard. Mater. 178 (2010) 385–389.
[16] P.R. Shukla, H.Q. Sun, S.B. Wang, H.M. Ang, M.O. Tadé, Catal. Today 175 (2011) 380–385.
[17] K. Chan, W. Chu, Water Res. 43 (2009) 2513–2521.
[18] Y. Ding, L. Zhu, A. Huang, X. Zhao, X. Zhagn, H. Tang, Catal. Sci. Technol. 2 (2012) 1977–1984.
[19] P.R. Shukla, S. Wang, K. Singh, H.M. Ang, M.O. Tadé, Appl. Catal. B: Environ. 99 (2010) 163–169.
[20] P.R. Shukla, H. Sun, S. Wang, H.M. Ang, M.O. Tadé, Catal. Today 175 (2011) 380–385.
[21] P.R. Shukla, S. Wang, H. Sun, H.M. Ang, M.O. Tadé, Appl. Catal. B: Environ. 100 (2010) 529–534.
[22] H. Sun, H. Tian, Y. Hardjono, C.E. Buckley, S. Wang, Catal. Today 186 (2012) 63–68.
[23] J. Zou, J. Ma, L. Chen, X. Li, Y. Guan, P. Xie, C. Pan, Environ. Sci. Technol. 47 (2013) 11685–11691.
[24] Y. Wang, W. Chu, Water Res. 45 (2011) 3883–3889.
[25] Y. Pan, W. Chen, S. Lu, Y. Zhang, Dyes Pigments 66 (2005) 115–121.
[26] W. Lu, N. Li, S. Bao, W. Chen, Y. Yao, Carbon 49 (2011) 1699–1709.
[27] A.B. Sorokin, Chem. Rev. 113 (2013) 8152–8191.
[28] V. Iliev, A. Ileva, J. Mol. Catal. A: Chem. 103 (1995) 147.
[29] J. Yang, D. Mu, Y. Gao, J. Tan, A. Lu, D. Ma, J. Nat. Gas Chem. 21 (2012) 265–269.
[30] E. Jubete, K. Żelechowska, O.A. Loaiza, P.J. Lamas, E. Ochoteco, K.D. Farmer, K.P. Roberts, J.F. Biernat, Electrochim. Acta 56 (2011) 3988–3995.
[31] M.A. Zanjanchi, A. Ebrahimian, M. Arvand, J. Hazard. Mater. 175 (2010) 992–1000.
[32] C. Shen, C. Song, L. Zang, X. Kang, Y. Wen, W. Liu, L. Fu, J. Hazard. Mater. 177 (2010) 560–566.
[33] W. Lu, W. Chen, N. Li, M. Xu, Y. Yao, Appl. Catal. B: Environ. 87 (2009) 146–151.
[34] W. Chen, W. Lu, Y. Yao, M. Xu, Environ. Sci. Technol. 41 (2007) 6240–6245.
[35] A.D. Bokare, R.C. Chikate, C.V. Rode, K.M. Paknikar, Environ. Sci. Technol. 41 (2007) 7437–7443.
[36] S. Liang, L. Zhao, B. Zhang, J. Lin, J. Phys. Chem. A 112 (2008) 618–623.
[37] L. Hu, F. Yang, W. Lu, Y. Hao, H. Yuan, Appl. Catal. B: Environ. 134–135 (2013) 7–18.
[38] Y. Yao, Z. Yang, H. Sun, S. Wang, Ind. Eng. Chem. Res. 51 (2012) 14958–14965.
[39] H. Eibenberger, S. Steenken, P.O' Neill, D. Schulte-Frohlinde, J. Phys. Chem. 82 (1978) 749–750.
[40] S.T. Martin, A.T. Lee, M.R. Hoffmann, Environ. Sci. Technol. 29 (1995) 2567–2573.
[41] Z. He, S. Song, H. Ying, L. Xu, J. Chen, Ultrason. Sonochem. 14 (2007) 568–574.
[42] L. Xu, J. Wang, Environ. Sci. Technol. 46 (2012) 10145–10153.
[43] P. Maruthamuthu, P. Neta, J. Phys. Chem. 81 (1977) 937–940.
[44] Y. Huang, Y. Huang, J. Hazard. Mater. 167 (2009) 418–426.
[45] T. Vickerstaff, The Physical Chemistry of Dyeing, 2nd ed., Oliver and Boyd, London, 1954.